ISSN 0036-0244, Russian Journal of Physical Chemistry A, 2016, Vol. 90, No. 9, pp. 1879–1884. © Pleiades Publishing, Ltd., 2016.
Original Russian Text © S.V. Shevkunov, 2016, published in Zhurnal Fizicheskoi Khimii, 2016, Vol. 90, No. 9, pp. 1402–1408.

PHYSICAL CHEMISTRY
OF SURFACE PHENOMENA

Effect of Hydrophilic Walls on the Hydration of Sodium Cations in Planar Nanopores

S. V. Shevkunov

Peter the Great St. Petersburg Polytechnic University, St. Petersburg, 195251 Russia
e-mail: shevk54@mail.ru

Received August 18, 2015

Abstract—A computer simulation of the structure of Na^+ ion hydration shells with sizes in the range of 1 to 100 molecules in a planar model nanopore 0.7 nm wide with structureless hydrophilic walls is performed using the Monte Carlo method at a temperature of 298 K. A detailed model of many-body intermolecular interactions, calibrated with reference to experimental data on the free energy and enthalpy of reactions after gaseous water molecules are added to a hydration shell, is used. It is found that perturbations produced by hydrophilic walls cause the hydration shell to decay into two components that differ in their spatial arrangement and molecular orientational order.

Keywords: hydration, ion, nanopore, computer simulation
DOI: 10.1134/S0036024416080276

INTRODUCTION

The hydration of ions in nanoscopic pores plays a key role in activating the mechanisms of interaction of ions with imperfect surfaces of various morphologies under the natural conditions of humid air. The most likely sites on which the clustering of gaseous water molecules on solid surfaces occurs, initializing chemical reactions with impurity components, the corrosion of the surface, and its dissolution in a growing microdrop, are surface defects in the form of steps, wedge-shaped fractures, and planar cracks.

Theoretical studies on the effect water vapor has on the chemical transformation of pollutants in the natural atmosphere have attracted growing attention over the last decade, due to the wide range of air pollution problems created by industrial effluents [1–3]. At the same time, hydration in nanoscopic pores remains a virtually unexplored area [4, 5]. There have been several studies on the hydration of ions in nanopores completely filled with water [6–11], and considerably fewer works on hydration in pores interacting with water vapor. In [12–14], the hydration of a singly-charged Cl^- anion in a planar nanopore with structureless hydrophobic walls in contact with water vapor was studied by means of computer simulation. Similar studies for a Na^+ cation in a planar nanopore were conducted in [15, 16]. Characteristics of the structure and growth mechanism of the hydration shell of a Na^+ cation in a planar nanopore that are determined by the hydrophilic walls of the nanopore are studied in this work.

CALCULATION METHOD

A continuum approximation approach cannot be used to study the hydration shells of ions, due to the extremely small size of the system (comparable to the radius of intermolecular correlations). The discrete molecular structure must in this case be explicitly considered. At the same time, the lack of spatial homogeneity complicates the use of integral equations as in 3D systems [17–19], and the lack of ideality excludes the use of virial expansions [20–22]. Computer simulation is in this case a reliable means of theoretical studies.

The Monte Carlo method is based on the fundamental principles of statistical mechanics and is free of mean-field theory approximations; exchanges of energy and particles with the environment are described explicitly. For our intermolecular interaction, the statistical part of the problem is generally solved with precision by considering all spatial correlations. The weaknesses of this method are the numerical form of the final results and the need to repeat laborious computer calculations many times if we want to cover a finite interval of conditions.

A detailed multicenter model of intermolecular interactions, ICP(SPC) (ions + covalent bonds + polarization, based on SPC geometry), [23–25] was used in our calculations. Along with the Coulomb, exchange, and dispersion interactions, the ICP(SPC) model explicitly considers the polarization of molecules in an ion's field and the polarization of an ion in the electric field of molecules, along with many-body interactions of the covalent type and the effects of par-

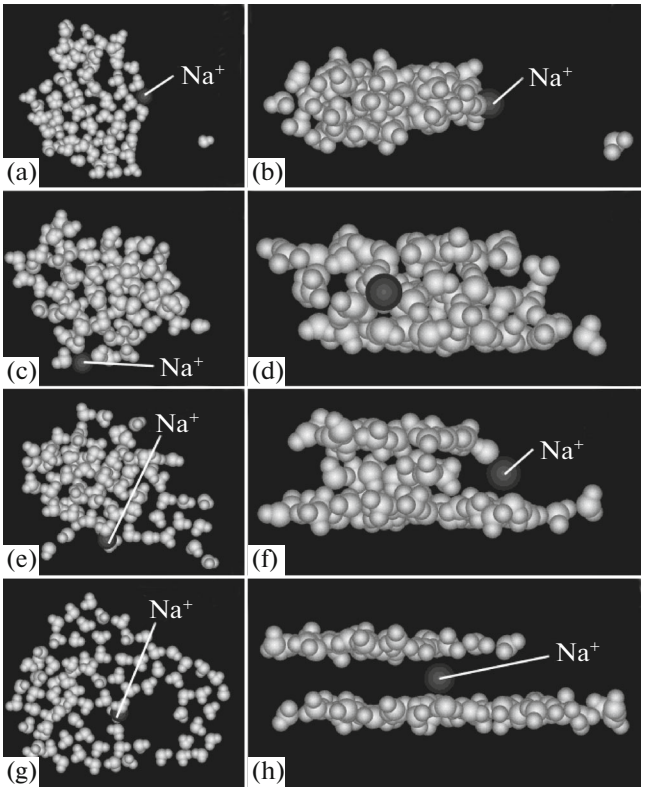

Fig. 1. An Na^+ ion hydrated by eight water molecules in a model planar pore with a width of 0.7 nm and hydrophobic and hydrophilic structureless walls at a temperature of 298 K. The energies of bonding interaction with the walls are (a and b) 0, (c and d) $2.5k_BT$, (e and f) $5k_BT$, and (g and h) $10k_BT$; the width of the potential well for water molecules on the walls is 0.1 nm. The views are in the directions (a, c, e, and g) perpendicular and (b, d, f, and h) parallel to the plane of the pore.

tial charge transfer. Numerical values of the model parameters were determined with an accuracy of up to tenths of the k_BT value via consecutive iterations due to the condition of reproducibility of the experimental free energies and enthalpies [26] of the first reactions describing the addition of gaseous water molecules to the ion's hydration shell, $Na^+(H_2O)_{n-1} + H_2O \rightarrow Na^+(H_2O)_n$.

The Gibbs free energy and entropy were calculated using a bicanonical statistical ensemble (BSA) [27–32]. The BSA method yields absolute values of the free energy, not relative values as in most alternative approaches [33]. This allows us to follow the entire cycle of the formation of a cluster from water vapor, starting at extremely small sizes.

A compact form for describing many-body interactions is found in the ICP(SPC) model, which ensures linear growth of the required computation time at each step of the Monte Carlo procedure in line with number of molecules N, but not quadratic growth as when using the standard formula for many-body interactions. Comparative calculations show [34, 35] that ignoring many-body interactions results in the accumulation of considerable errors in the work of formation as the hydration shell of an atomic ion grows, and greatly distorts the picture of the system's thermodynamic behavior, both in the rate of hydration and the equilibrium concentration of clusters in the water vapor.

RESULTS AND DISCUSSION

Computer calculations in a canonical statistical ensemble containing from 1 to 100 molecules were performed by the Monte Carlo method at a temperature of 298 K. Equilibrium characteristics were averaged over 200 million configurations. The procedure of a gradual escalation in the number of molecules with steps of one molecule was used. Each time a molecule was added to the system, it was thermalized over 100 million calculation steps. One step of the Markov stochastic process consisted of the spatial shift and rotation of a randomly selected molecule by a random shift vector and a random angle of rotation, respectively. The probabilities of a transition to a new configuration are calculated using a random number generator and ensure an equilibrium Gibbs distribution over all configurations. From the arrays obtained in this manner, the particle coordinates are randomly selected and processed in order to develop three-dimensional color images. Processing computer programs allow us to rotate the images, to view them from different angles, and to change the visual perspective and magnification.

The possibility of working with 3D images on a computer screen allows us to gain a better idea of the molecular structure of the system, though the main patterns are observable even on planar projections. Examples of such projections in black and white are given in Fig. 1. The view in the direction perpendicular to the plane of the pore is shown in the left column, and the same configuration in the direction along the plane of the pore is on the right column. There is no attraction to the walls in the figures given in the first row (Figs. 1a and 1b). In the rest of the images, the hydrophilicity of the walls increases as we move from the top of the columns to the bottom.

Regardless of the degree of hydrophilicity of the walls, it is clearly seen in all the images that the Na^+ ion is pushed out of the cluster and appears to be on the periphery (Figs. 1a–1g). The expulsion of atomic ions from their own hydration shells in bulk water vapor was observed for the first time for the Cl^- ion and was attributed to its high electric polarizability [36–38]. However, the same phenomenon was observed in later studies for the Na^+ ion, which does

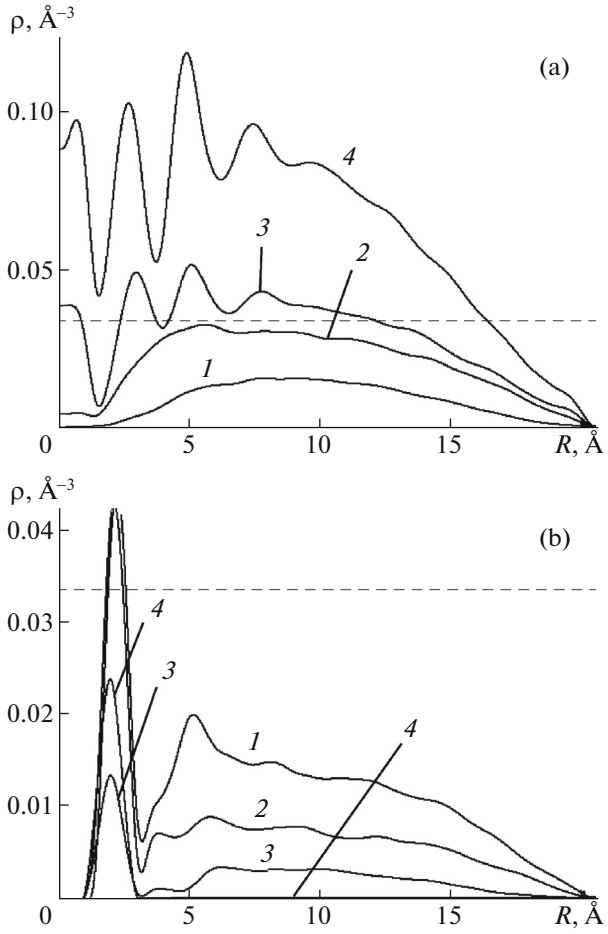

Fig. 2. Equilibrium radial distributions of eighty water molecules at 298 K in the field of the Na^+ ion in a model planar pore 0.7 nm wide with hydrophobic and hydrophilic structureless walls at distances of (a) 0.05 nm and (b) 0.25 nm from the wall. The energies of bonding interaction with the walls are (*1*) 0, (*2*) $2.5k_BT$, (*3*) $5k_BT$, and (*4*) $10k_BT$; the width of the potential well for water molecules on the walls is 0.1 nm; and distance R is measured from the normal to the plane of the pore, which passes through the center of the ion fixed between the walls. The density of water under normal conditions is shown by the dashed lines.

not have as high a polarizability as the Cl^- ion in either bulk water vapor [34, 39] or a planar pore with hydrophobic walls [15]. The expulsion of an ion drastically affects the thermodynamic stability of its hydration shell [39]. The results from the above observations allow us to conclude that the main reason for the expulsion effect is the destruction of hydrogen bonds between molecules by the strong electric field of the ion and a consequent increase in the energy of intermolecular interactions; polarization forces only accelerate this process. The network of hydrogen bonds is destroyed to a minimum extent when the ion is located on the cluster's surface. The obtained data show that the expulsion of ions from their own hydration shells occurs regularly and under the conditions of hydrophilic walls.

Upon an increase in hydrophilicity, a molecular cluster in an ionic field decays into two spots that spread out on the surface of the walls above and below the ion (Fig. 1h). The spots are mainly positioned not above each other, but with some relative shift arising from the mutual repulsion of spots polarized in opposite directions. This polarization is caused by the strong electric field of the ion.

Analysis of the images shows that two components can be distinguished in the molecular structure of the cluster formed near the ion. The first consists of water molecules located outside the area of attraction to the walls; the second, of molecules adhering to the walls. Molecules of the first type are trapped exclusively by the ionic field, while molecules of the second type form monomolecular spots whose integrity is due to the combined action of the attraction forces from both the walls and the ion.

When the width of the pores is increased to more than 1 nm, the first component is transformed into elongated structures linking the ion with the spots on the wall surface (these images are not shown in this work). The water molecules in these links are aligned by their oxygen atoms in the direction of the ion and form chains fastened on the molecules making up the spots on the walls by means of hydrogen bonds. The ion's hydration shell under the conditions of highly hydrophilic walls takes the form of two symmetrically positioned mushrooms with the stems resting on the ion and the caps adhering to the pore walls.

Monomolecular spots have a pronounced layered structure in the plane of the walls that is barely discernable in separate configurations but can be identified from oscillations of the radial distributions of the local density of molecules obtained by averaging over the configurations (Fig. 2). The layering depends strongly on the hydrophilicity of the walls and becomes more extensive as it grows. If there is no layering under the conditions of hydrophobic walls, as seen from the smooth form of curve *1* in Fig. 2a, and only weak traces of oscillations are distinguished in the field of weakly hydrophilic walls (curve *2*), strong structuring of the spots on walls with medium (curve *3*) and high (curve *4*) hydrophilicity is observed. The distances between adjacent maxima on the radial distributions correspond to those between adjacent radial layers in the spots (approximately 0.2 nm). As can be seen from the patterns of the spots, the water molecules in them form a network of interlinked cycles. The size of the cycles varies from three to six molecules, while five-membered cycles are observed more frequently than others (Fig. 1g). The structuring of the cluster under conditions of sufficiently strong hydrophilic properties occurs even on structureless walls.

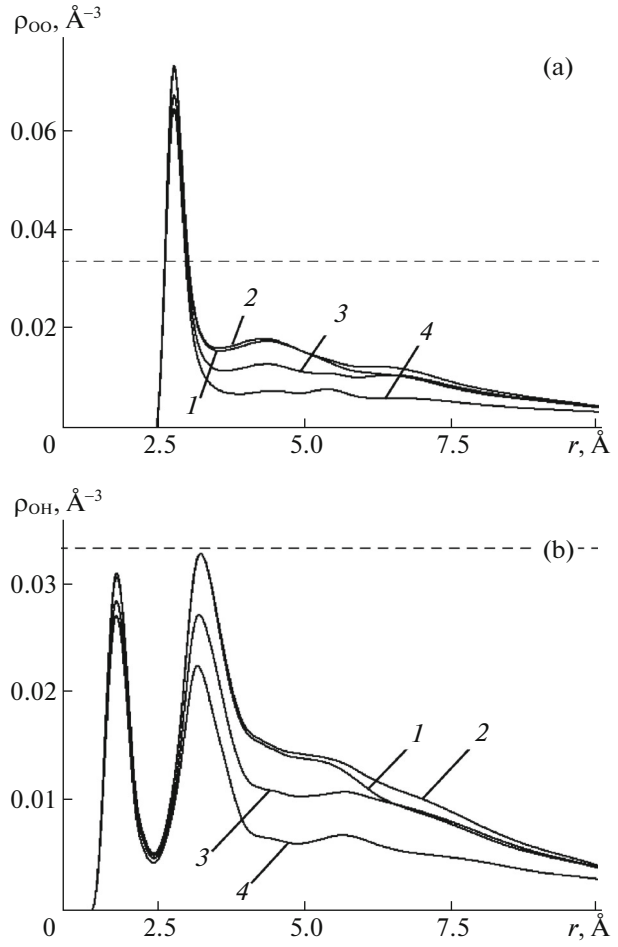

Fig. 3. (a) Oxygen–oxygen and (b) oxygen–hydrogen binary correlation functions of sixty water molecules in the field of a Na^+ ion at 298 K in a model planar pore 0.4 nm wide at different degrees of the walls' hydrophilicity. The energies of bonding interactions with the walls and the numbering of the curves are the same as in Fig. 2.

The thickness of a spot on a wall's surface is a single molecular layer. This can be seen from the sharp drop in density and reduction in the area occupied by water molecules at a distance of 0.25 nm from the wall (Fig. 2b). In contrast, if the density of the water molecules in the spot on its surface increases along with hydrophilicity (curves *1–4* in Fig. 2a are positioned above one another), the density falls at a distance of 0.25 nm (curves *1–4* in Fig. 2b are arranged in reverse order). The spatial distribution of the molecules in this case differs qualitatively; i.e., there is a relatively narrow maximum at the distance of interaction from the ion, followed by a weakly-structured area with a low concentration of water molecules at distances corresponding to $R > 0.3$ nm. This form of distribution is typical of the narrow stem of a mushroom-like cluster surrounded by a loose, weakly-structured gaseous medium. The thickness of this molecular linking between an ion and a spot on the wall varies from one to several molecular layers when the pores are filled by water molecules. It should be noted that the height of the first maximum changes non-monotonically: the maximum in curve *3* is lower than the maxima in both curves *2* and *4*.

In addition to layered spatial ordering in the radial direction, a layered structure in pores more than 1 nm wide also forms along the molecular link in the direction from the ion to the wall.

Earlier studies showed the high stability of binary atom–atom correlation functions with respect to variations in the thermodynamic conditions of the condensed water phase. No sharp changes in the form of one-time atom–atom correlation functions are observed even upon the crystallization of water. Crystallization in in situ experiments is detected from abrupt changes in the kinetic parameters, e.g., the coefficient of viscosity or the elastic shear modulus. The kinetic coefficients are expressed via two-time velocity autocorrelation functions; these are calculated using various integration techniques for equations describing the motion of particles in real time. The kinetic coefficients cannot be calculated by the Monte Carlo method in its standard version.

We might expect that the one-time atom–atom correlation functions in the ion's hydration shell would be resistant to the influence of hydrophilic walls as well. Computer simulation shows that stability of the correlation functions is actually observed, but only at the contact distances. The oxygen–oxygen and oxygen–hydrogen correlation functions of the water molecules in the field of the Na^+ ion inside a nanopore are shown in Fig. 3 for different degrees of the hydrophilicity of the walls. The functions are normalized as

$$\int_0^\infty \rho_{OO}(r)4\pi r^2 dr = \int_0^\infty \rho_{OH}(r)4\pi r^2 dr = N - 1,$$

where N is the number of water molecules in the system. The physical meaning of correlation function $\rho_{OO}(r)$ is the mean volumetric density of water molecules at distance r from a randomly selected molecule. Correlation function $\rho_{OH}(r)$ is the volumetric density of oxygen atoms at distance r from a randomly selected hydrogen atom. The volumetric density is averaged over all directions and thus contains no information on the distribution anisotropy.

Curve *1* was obtained for hydrophobic walls; the remaining curves, for hydrophilic walls. The first maximum in Fig. 3b reflects the formation of hydrogen bonds. Its position corresponds to the length of a hydrogen bond, and the area under the curve corresponds to the mean number of hydrogen bonds for each hydrogen atom of a water molecule. The total number of hydrogen bonds in which a water molecule acts as a donor is twice as high. To determine the total

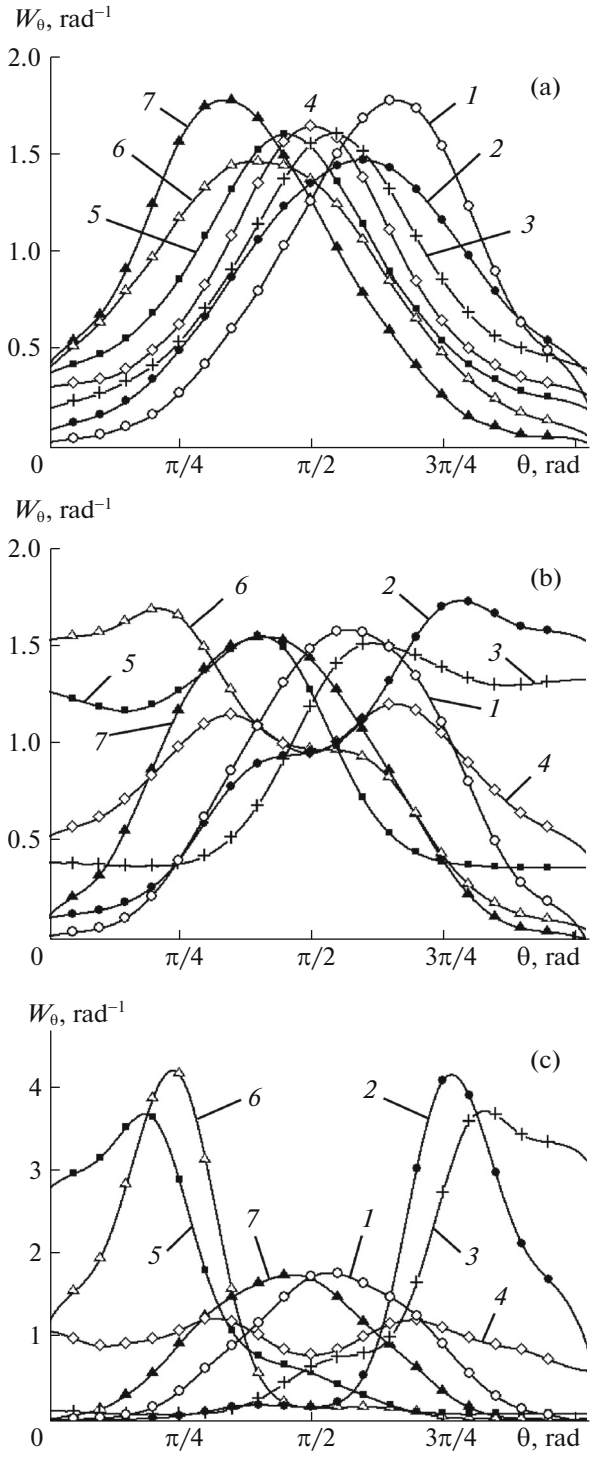

Fig. 4. Angular distributions of twenty water molecules in the field of a Na^+ ion in a model planar pore at distances of (*1*) 0.05, (*2*) 0.15, (*3*) 0.25, (*4*) 0.35, (*5*) 0.45, (*6*) 0.55, and (*7*) 0.65 nm from the wall, as in Fig. 2. The energies of bonding interaction with the walls are (a) 0, (b) $2.5k_BT$, and (c) $5k_BT$; θ is the angle between the normal to the plane of the inner walls and the dipole moment of a water molecule.

number of hydrogen bonds formed by a water molecule and its neighboring molecules, we must add the number of hydrogen bonds in which the water molecule acts as an acceptor. Since two water molecules are involved in the formation of one hydrogen bond, the mean number of hydrogen bonds per one molecule is half as great. The area under the first maximum of $\rho_{OH}(r)$ is thus proportional to the mean number of hydrogen bonds in the system. As we may conclude from a comparison of curves *1–4* in Fig. 3b, a hydrophilic wall leads to the breaking of some hydrogen bonds, but the effect is negligible in quantitative terms. The mean length of hydrogen bonds in this case does not change.

Hydrophilic walls have a considerable effect on spatial correlations at medium and long distances. As seen from a comparison of curves *1–4* in Fig. 3, the effect hydrophilic walls have at medium distances in the range of 0.3 to 1 nm gives rise to a marked reduction in the correlation functions. In view of the normalization condition, such a reduction should be compensated for by an increase at greater distances outside the range given in Fig. 3. Water molecules are thus found more often at greater distances under the conditions of hydrophilic walls. Some of the hydrogen bonds between them break, so the system becomes looser in general.

Hydrophilic walls exert their greatest effect on the molecular orientational order. The angular distributions of molecules under the conditions of (a) hydrophobic, (b) weakly hydrophilic walls, and (c) walls with a medium degree of hydrophilicity are shown in Fig. 4. Certain tendencies are observed in the evolution of the orientational order upon an increase in the hydrophilicity of walls. When there is no attraction to the walls (Fig. 4a), the distributions of the orientations of the dipole moments of water molecules have the shape of an almost perfect bell. In the field of hydrophilic walls (curve *4* in Fig. 4b), the angular distribution in a layer between walls becomes bimodal; i.e., water molecules with deviations of their dipole moments in the direction of both walls predominate over those whose dipole moments are parallel to the walls.

In the subsequent layers closest to the ion, the number of water molecules with dipole moments aligned parallel to the normal of the wall planes increases drastically. This can be seen from the rise of curves *3* and *5* in Fig. 4b at angles near $\theta = \pi$ and $\theta = 0$, respectively. This effect is even more profound on curves *2* and *6*, which correspond to molecules located closer to the walls. At the same time, the orientation of water molecules differs qualitatively near contact with the walls; curves *1* and *7* associated with the molecules adhering to the wall have maxima close to $\theta = \pi/2$, i.e., almost parallel to the plane of the pore. As can be seen from a comparison of the positions of curves *1* and *7* in Figs. 4a and 4b, the most

likely orientation of the dipole moments of water molecules in a monomolecular layer in contact with a wall is close to the direction parallel to the wall upon an increase in its hydrophilicity.

Under conditions of medium wall hydrophilicity (Fig. 4b), the orientational order allows us to identify two parts in the system: the molecules of a monomolecular layer in contact with the walls are positioned almost parallel to the wall by their dipole moments (curves *1* and *7*), while the orientation of the dipole moments of the rest of molecules (curves *2*–*6*) tends toward the normal. Upon an increase in hydrophilicity, the division of the system is even more striking: the most likely orientation of the first part of the molecules is close to the direction along the walls; the orientation of the second part, close to perpendicular.

CONCLUSIONS

Our data show that the effect hydrophilic walls have on the hydration shell of an ion in a planar nanopore leads to it decaying into two parts that differ in their spatial arrangement and orientation. It would be expected that the observed structural features of the hydration shell affect its thermodynamic behavior and thermal stability.

ACKNOWLEDGMENTS

This work was supported by the Russian Foundation for Basic Research, project no. 13-03-00062-a.

REFERENCES

1. G. M. Hartt, G. C. Shields, and K. N. Kirshner, J. Phys. Chem. A **112**, 4490 (2008).
2. N. Salmi, N. Runeberg, L. Halonen, J. R. Lane, and H. G. Kjaergaard, J. Phys. Chem. A **114**, 4835 (2010).
3. J. Clark, A. M. English, J. C. Hansen, and J. S. Francisco, J. Phys. Chem. A **112**, 1587 (2008).
4. R. M. Lynden-Bell and J. C. Rasaiah, J. Chem. Phys. **105**, 9266 (1996).
5. G. Lakatos and G. N. Patey, J. Chem. Phys. **126**, 024703 (2007).
6. K. Kiyohara, T. Sugino, and K. Asaka, J. Chem. Phys. **132**, 144705 (2010).
7. T. A. Beua, J. Chem. Phys. **132**, 164513 (2010).
8. P. Taboada-Serrano, S. Yiacoumi, and C. Tsouris, J. Chem. Phys. **123**, 054703 (2005).
9. Ch.-H. Hou, P. Taboada-Serrano, S. Yiacoumi, and C. Tsouris, J. Chem. Phys. **128**, 044705 (2008).
10. C. Desgrange and J. Delhommelle, Mol. Simul. **34**, 177 (2008).
11. M. E. Selvan, D. J. Keffer, S. Cui, and S. J. Paddison, Mol. Simul. **36**, 568 (2010).
12. S. V. Shevkunov, Colloid. J. **76**, 490 (2014).
13. S. V. Shevkunov, Russ. J. Electrochem. **50**, 1118 (2014).
14. S. V. Shevkunov, Russ. J. Electrochem. **50**, 1127 (2014).
15. S. V. Shevkunov, Russ. J. Phys. Chem. A **88**, 1744 (2014).
16. S. V. Shevkunov, Russ. J. Phys. Chem. A **88**, 2165 (2014).
17. J. G. Kirkwood and J. C. Poirier, J. Phys. Chem. **58**, 591 (1954).
18. J. C. Rasaiah and H. L. Friedman, J. Chem. Phys. **48**, 2742 (1968); J. Chem. Phys. **50**, 3965 (1969).
19. D. D. Carley, J. Chem. Phys. **46**, 3783 (1967).
20. J. E. Mayer, J. Chem. Phys. **18**, 1426 (1950).
21. E. Salpeter, Ann. Phys. (N.Y.) **5**, 183 (1958).
22. E. J. Meeron, J. Chem. Phys. **28**, 630 (1958).
23. S. V. Shevkunov, Colloid. J. **66**, 216 (2004).
24. S. V. Shevkunov, Russ. J. Electrochem. **49**, 228 (2013).
25. S. V. Shevkunov, Colloid. J. **76**, 753 (2014).
26. M. Arshadi, R. Yamdagni, and P. Kebarle, J. Phys. Chem. **74**, 1466 (1970).
27. S. V. Shevkunov, High Temp. **51**, 79 (2013).
28. S. V. Shevkunov, Russ. J. Phys. Chem. A **85**, 1584 (2011).
29. S. V. Shevkunov, Colloid. J. **67**, 497 (2005).
30. S. I. Lukyanov, Z. S. Zidi, and S. V. Shevkunov, Chem. Phys. **332**, 188 (2007).
31. S. I. Lukyanov, Z. S. Zidi, and S. V. Shevkunov, Fluid Phase Equilib. **233**, 34 (2005).
32. S. V. Shevkunov, J. Exp. Theor. Phys. **108**, 447 (2009).
33. A. P. Lyubartsev, A. A. Martsinovski, S. V. Shevkunov, and P. N. Vorontsov-Velyaminov, J. Chem. Phys. **96**, 1776 (1992).
34. S. V. Shevkunov, Russ. J. Phys. Chem. A **83**, 972 (2009).
35. S. V. Shevkunov, Colloid. J. **71**, 406 (2009).
36. C. J. Burnham, M. K. Petersen, T. J. F. Day, et al., J. Chem. Phys. **124**, 024327 (2006).
37. D. H. Herce, L. Perera, T. A. Darden, and C. Sagui, J. Chem. Phys. **122**, 024513 (2005).
38. S. Yoo, Y. A. Lei, and X. C. Zeng, J. Chem. Phys. **119**, 6083 (2003).
39. S. V. Shevkunov, Colloid. J. **73**, 275 (2011).

Translated by O.N. Kadkin